Techno-economic analysis on recent heterogeneous catalysts for ammonia synthesis

Masaki Yoshida[†], Takaya Ogawa[†,*], Keiichi N. Ishihara
Graduate School of Energy Science, Kyoto University, Yoshida-honmachi, Sakyo-ku, Kyoto, 606-8501, Japan
*Corresponding author.
E-mail address: ogawa.takaya.8s@kyoto-u.ac.jp (T. Ogawa).

Abstract

The economic performance of recently developed catalysts for ammonia synthesis, $Ru/Ca(NH_2)_2$ and Ru/Pr_2O_3, are evaluated by process simulation using ASPEN Plus. The results show that catalyst costs are high due to expensive ruthenium; thus, the catalysts' lifetime significantly influences the total cost. Besides, the new catalysts are advantageous when the electricity cost is high and the production scale is small, which are the characteristics of the case in which renewable energy is employed. Finally, the future direction of the catalyst developments is discussed.

Introduction

Ammonia is inevitable for modern human lives as an artificial nitrogen fertilizer and is the second most common chemical produced worldwide.[1] Ammonia production is more than 182 million tonnes in 2019 and is expected to increase by 4% during the next four years.[2] The ammonia synthesis occupies 1-2% of the whole energy consumption of human beings, indicating the enormous energy-consuming process.[3] Currently, hydrogen and energy sources for industrial ammonia production are fossil fuels.[4] Thus, for a sustainable society in the future, “green ammonia” should be synthesized from the hydrogen gas prepared by water electrolysis based on renewable energy.

Furthermore, ammonia is promising as a renewable energy carrier because it readily becomes a liquid state under less than 10 bar at room temperature, and liquid ammonia has a high energy density in weight and volume.[5-8] Ammonia-fueled power generation technology is being established.[9,10] The smaller volume results in less space in the fuel tank, and the smaller weight requires less energy to transport fuels together. Furthermore, product of ammonia after usage is nitrogen gas, which can be emitted into the air without pollution. And also, nitrogen gas can be obtained everywhere from the air. It means, after the utilization of ammonia, no need to recover and send back nitrogen gas to the location that generates hydrogen from renewable energy, which omits the cost and energy for recovery and transportation.[11-14] Moreover, a product of ammonia after usage is nitrogen gas, which can be emitted into the air without pollution. And also, nitrogen gas can be obtained everywhere from the air. It means, after utilizing ammonia, no need to recover and send back nitrogen gas to the location that generates hydrogen from renewable energy, which omits the cost and energy for recovery and transportation.[11-14] Therefore, liquid ammonia is suitable as a portable fuel and is beneficial to compensate for the power in the transport sector, accounting for roughly 30% of the world’s energy consumption.[15] The market size of ammonia has an enormous potential to expand in the near future.

Ammonia is produced through the following exothermic reaction: $N_2 + 3H_2 \rightarrow 2NH_3$ $\Delta H = -92$ kJ/mol.[16] Therefore, the lower temperature and higher pressure are favorable in equilibrium. However, the temperature must be elevated to accelerate the reaction at extremely high pressure: 350−525 °C and 100−300 bar.[17] Then, the equipment, including reactors and compressors, is much more expensive to endure the severe condition. These costs are usually

reduced by the economy of scale,[18] and thus the ammonia production plant has been generally large, e.g., 1000 tonnes/day.[19] The business model of centralized production and distribution to local areas has been successful for a long time. However, poor infrastructure for transport, such as feeders roads linking main cities to other regions of Zambia, Tanzania, Ghana, and Nigeria, increases the transaction cost, and farmers in these areas cannot obtain ammonia at an affordable price.[20,21] It results in low efficiency of food production and increases hunger.

Furthermore, the harsh condition requires significant time for the start-up, 30 hours at least.[22,23] It is fatal to utilize renewable energy due to its time variability. If the synthesis of ammonia at mild reaction conditions is achieved, it is possible to produce green ammonia using water and renewable energy and employ ammonia as an energy carrier. Moreover, it enables producing ammonia locally on a small scale and supplying it to local areas without transport cost. The mild reaction condition is essential to solving the above issues.

In recent years, the catalysts for ammonia synthesis have been remarkably redeveloped, starting with the report of Ru supported by an electride in 2012.[24] Several catalysts supported on not only electrides but nitrides and hydrides or without supports have also been reported one after another, which have high activity under mild reaction conditions.[25-31] Homogeneous catalysts for ammonia synthesis at room temperature and atmospheric pressure have also continued to develop since 2003.[32-37] These catalysts are very promising in solving the problems mentioned above. However, to the best of our knowledge, no research has investigated how economically advantageous these catalysts are in a process that correctly reflects their surprisingly high performance. There are numerous examples of evaluating the performance of ammonia synthesis loops. Still, they employ conventional iron-based catalysts or assume unrealistic catalytic activities such as reaching equilibrium immediately or that the reaction activity is constant under various conditions.[38-47] Investigating the cost structure of the synthetic loops with recent catalysts is crucial. It will reveal the conditions they are advantageous, how they can be made more economically viable, and the direction for future catalyst development.

In this study, we evaluate the economics of processes incorporating recently developed catalysts for ammonia synthesis. We focus on $Ru/Ca(NH_2)_2$[48] and Ru/Pr_2O_3,[49] which show remarkable activity and for which experimental data are abundantly reported to enable reaction modeling. The ammonia synthesis loops embedded with the two catalysts were modeled using ASPEN Plus©. A modified-Temkin model was employed to assess their catalytic activity correctly. In the reported paper, the available data were the test under the reaction conditions up to 10−30 bar,[48,49] but it is inferred that the target conditions for those catalysts are around 50 bar.[50] We extrapolated the low-pressure results and modeled them as data at 50 bar. The economic feasibility was evaluated at various scales, from small to large scale, and by varying the cases, such as using storage batteries to smooth out the time variability of renewable energy. The conditions under which the newly developed catalyst shows superiority were clarified, and guidelines for future catalyst development were discussed.

2. Method

2.1 Whole scheme of the ammonia synthesis loop

Figure 1 shows the system boundary of this study. An ammonia production plant consists of hydrogen and nitrogen production and an ammonia synthesis loop. We focused on the ammonia synthesis loop because the purpose was to evaluate the impact of the mild reaction condition achieved by $Ru/Ca(NH_2)_2$ and Ru/Pr_2O_3 on the ammonia synthesis loop. In addition, the loops with the commercialized iron-based catalysts, KM1R (Fe), and conventional Ru-based

catalyst, Ru/C,[51-53] were also investigated as a comparison. Although the cost of the hydrogen and nitrogen production process is inevitable, it does not change the conclusion of the comparison among all plants because the amount of hydrogen and nitrogen gas is the same. Therefore, the cost calculation for the ammonia synthesis loop is sufficient for the comparison (Figure 1).

Cryogenic air separation is suitable for preparing nitrogen gas because of the high purity of nitrogen,[39,54] since the catalysts for ammonia synthesis are readily poisoned by H_2O and O_2.[55] Pressure swing adsorption is not suitable because it cannot achieve high purity for the ammonia synthesis, although it seems preferable for small-scale production. We assumed to utilize the cold heat of O_2 and N_2 in the cryogenic air separation to cool down ammonia for the separation. Aspen Plus© was employed to simulate the whole processes of the ammonia synthesis loop. The loop was based on the template of the ammonia synthesis plant in Aspen Plus© with some modifications (Fig. 2).[56] The properties of gas and liquid were from the database in Aspen Plus©. The loop scales were 5−1000 tonnes/day. The inlet gas is the stoichiometric ratio of ammonia, $H_2/N_2 = 3$.

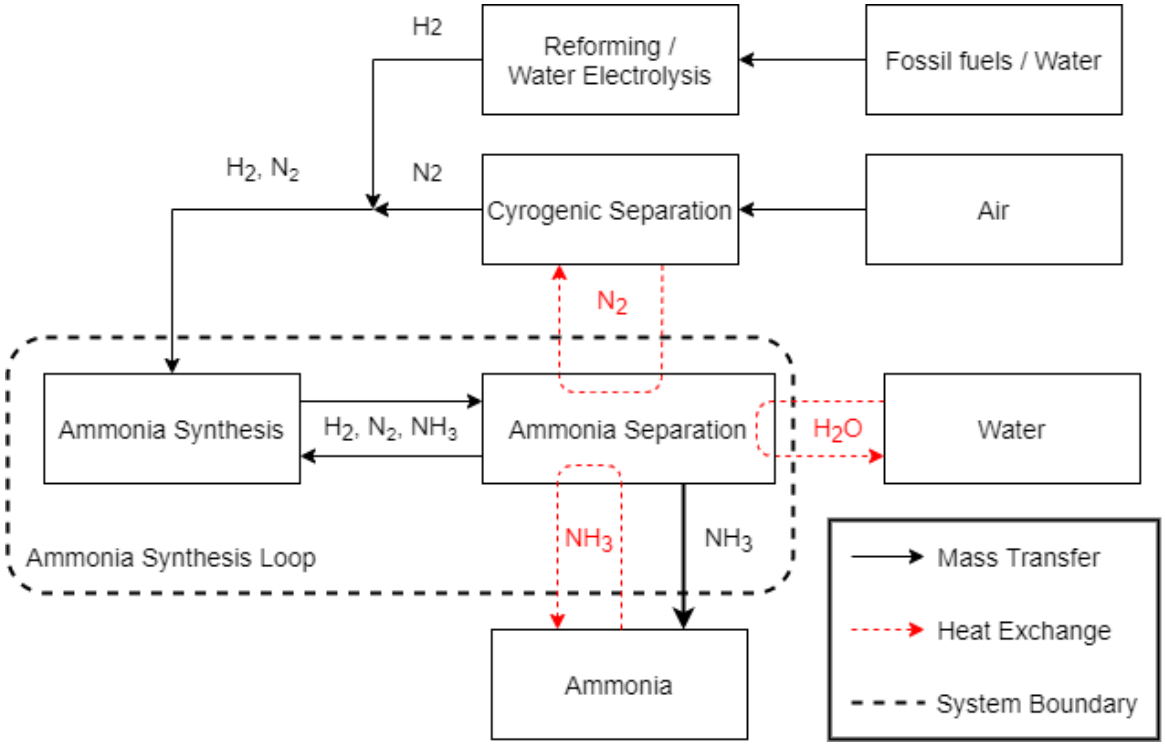

Fig. 1. The system boundary of this study, where the cost calculation was conducted for the ammonia synthesis loop.

2.2 Multi catalyst beds and cooling system

Reaction kinetics of $Ru/Ca(NH_2)_2$[48] and Ru/Pr_2O_3,[49] were modeled by the lab-scale experimental data in the temperature and pressure ranges shown in Table 1. For pressure, we extrapolated the model based on the available data at low pressure to reproduce the reaction performance at 50 bar since the catalysts are expected to be used at 50 bar in practical.[50] The operation temperature in the reactor needs to be elevated to accelerate the reaction, although ammonia synthesis is an exothermic reaction. It means that as the reaction proceeds, the temperature increases to be close to the equilibrium, and the reactivity slows down. Therefore, the reactor needs to cool down when the

temperature is too high. The plant generally employs a multi-bed reactor and removes the heat in the outlet of each reactor. The difference between inlet and outlet (ΔT) was kept less than 90 K for safety.[18] In this study, three beds system was applied because the three-bed reactor system was found to be the most efficient in terms of NH_3 production, energy savings, capital, and maintenance cost.[57] The three-bed reactor system consisted of three reactors and two heat exchangers (Fig. 2(b)). In the case that the ammonia concentration is close to equilibrium, the reaction rate slowdowns and redundantly increases the reactor volume, resulting in high cost. Hence, the general way to determine the volume was employed, which stops the reaction when the product concentration reaches 90% of the equilibrium under adiabatic conditions.[58] The reaction was stopped when the ΔT increased to = 90 K, or the ammonia concentration in a reactor reached 90% of the equilibrium, determining the reactor's volume. The reaction temperature ranges for each catalyst were determined by the optimization to obtain the lowest cost with the above criteria and available experimental data from literature.

Table 1 The reaction condition utilized for reaction modeling

Catalyst	Pressure [bar]	Inlet Temperature [°C]
KM1R (Fe-based)	150	400−500
Ru/C	100	350−500
Ru/C	50	350−470
Ru/Pr_2O_3	30	300−450
$Ru/Ba\text{-}Ca(NH_2)_2$	10	220−360

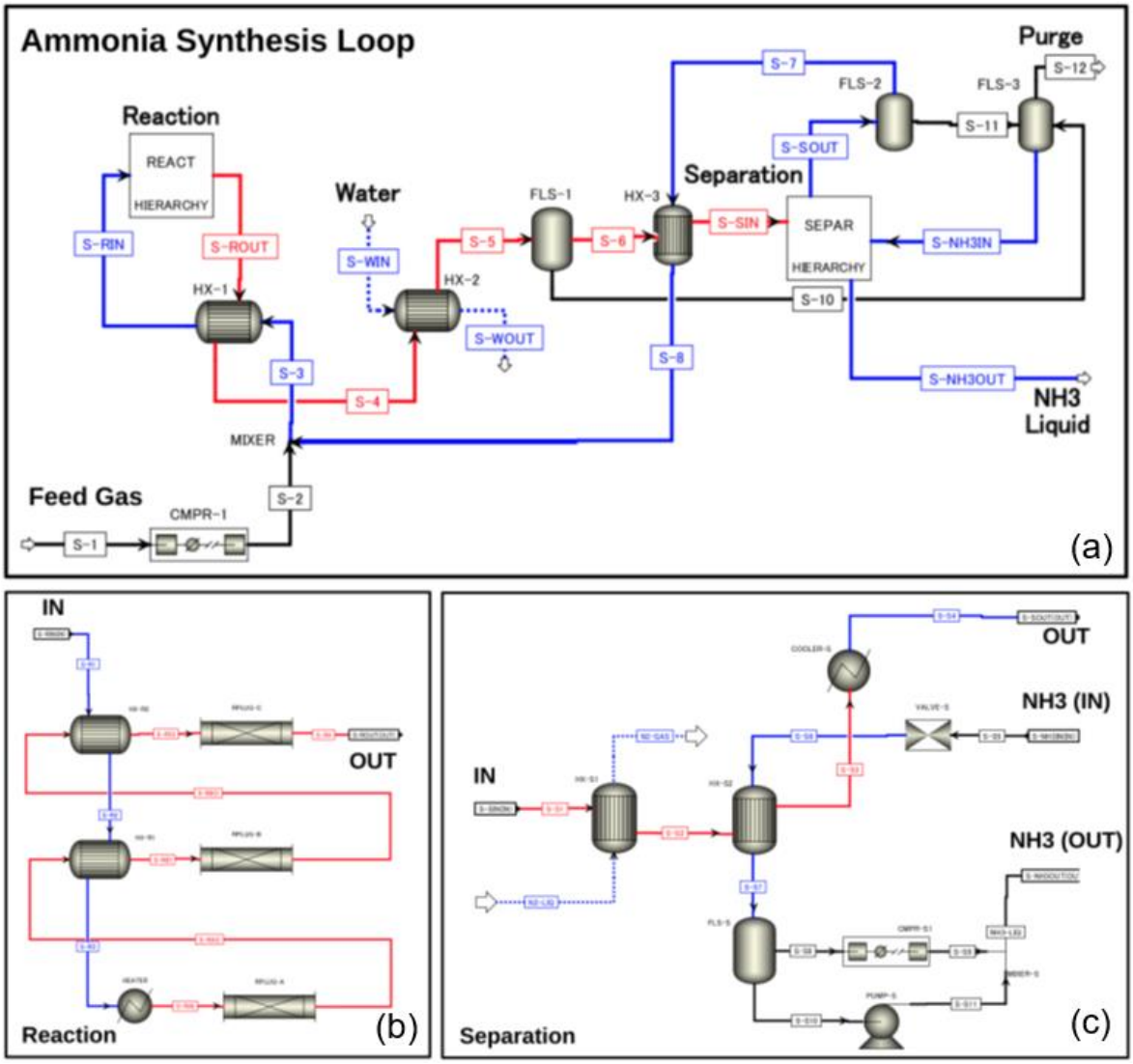

Fig. 2. (a) Overall layout of the ammonia synthesis loop simulation in Aspen Plus©. (b) Flowsheet of the ammonia synthesis process: the details of the "Reaction" block in the overall flowsheet. (c) Flowsheet of the ammonia refrigeration process for separation of the product NH_3: details of the "Separation" block in the overall flowsheet.

2.3 Separation of ammonia by refrigeration

The ammonia concentration at equilibrium is small under high temperatures. Then, plenty of H_2 and N_2 remains unreacted and needs to be recycled from the viewpoint of cost. For recycling, we employed a general method in ammonia synthesis, refrigeration under high pressure, to make ammonia liquid and separate the product liquid and the reactant gases. The refrigeration temperature was adjusted to bring the NH_3 molar concentration at the reactor inlet to 3 %, the typical value for the ammonia collection in the plant.[59] Water was utilized to initial cooling to room temperature (30 °C), and the cooled nitrogen gas in cryogenic air separation was used in the second. The pressure of the NH_3 product was released, and its latent heat and cold heat were utilized to lower the temperature, followed by the compression of the product to be liquid under 20 bar at room temperature, 30 °C (Fig. 2(c)). In the plant embedded with $Ru/Ca(NH_2)_2$ at 10 bar, the refrigeration process differs from others because the required temperature for cooling was too low, −33.3 °C, the boiling point of ammonia.

2.4 Kinetics in a reactor

Plenty of experimental kinetic data for KM1R is represented by the simple Temkin equation.[60-62] However, the Temkin equation cannot describe the experimental kinetic data for Ru-based catalysts well because the reaction over Ru-based catalysts is inhibited by hydrogen poisoning[63,64] while the reaction over Fe-based catalysts is inhibited by ammonia poisoning.[63] Buzzi et al. considered 23 possible kinetic models by the Langmuir-Hinshelwood-Hougen-Watson (LHHW) approach, separating the reaction into elementary reaction steps and expressing the overall reaction as the slowest step rate.[65] Rossetti et al. modified the Temkin equation to successfully represent the experimental kinetic data for Ru/C catalyst by the LHHW approach, which takes into account hydrogen poisoning.[63] The modified-Temkin equation under the condition of the feeding ratio $H_2/N_2 = 3$ is the following:

$$r_{NH_3} = k_f \frac{(a_{N_2})^n \left[\frac{(a_{H_2})^{3\alpha}}{(a_{NH_3})^{2n}}\right]^{\alpha} - \frac{1}{(K_a)^{2n}}\left[\frac{(a_{NH_3})^{2n}}{(a_{H_2})^{3n}}\right]^{1-\alpha}}{1 + K_{H_2}(a_{H_2})^{3nw_2} + K_{NH_3}(a_{NH_3})^{2nw_3}} \quad (1)$$

where α, w_2, w_3, and n are constants, r_{NH_3} is the reaction rate in $kmol_{NH_3}/hr/m^3$of catalyst beds, k_f is a kinetic constant of the forward reaction, K_{H_2} and K_{NH_3} are the adsorption equilibrium constants for hydrogen and ammonia, respectively. These parameters of are $Ru/Ca(NH_2)_2$ and Ru/Pr_2O_3 catalysts were modeled by the available experimental data (see Supplementary information) through the following equations:

$$k_f = k_0 \exp\left(-\frac{E_a}{RT}\right) \quad (2)$$

$$log_e K_{H_2} = -\frac{A_{H_2}}{R} + \frac{B_{H_2}}{RT} \quad (3)$$

$$log_e K_{NH_3} = -\frac{A_{NH_3}}{R} + \frac{B_{NH_3}}{RT} \quad (4)$$

where E_a is the activation energy, A_X and B_X (X = H_2 or NH_3) are the constant. E_as of the catalysts are referred to experimental data.[48,49] The equilibrium constant K_a was calculated according to Gillespie and Beattie:[60,63,66]

$$\log_{10} K_a = -2.691122 \log_{10} T - 5.519265 \times 10^{-5} T$$
$$+1.848863 \times 10^{-7} T^2 + \frac{2001.6}{T} + 2.6899 \quad (5)$$

For gases, the activity of a component can be expressed as follows:

$$a_i = \frac{f_i}{P^{\ominus}} \tag{6}$$

where, f_i is the fugacity of component i, and $P^{\ominus}$ is the standard pressure. Choosing $P^{\ominus}$ as equal to 1 atm, one can be written as:

$$a_i = f_i = \varphi_i y_i P \tag{7}$$

where φ_i is the fugacity coefficient of component i, y_i is the molar fraction of component i, P is the pressure in atm. We employed the fugacity coefficients calculated by Cooper and Shaw et al. for hydrogen and by Cooper and Newton for nitrogen and ammonia.[60,63,67,68]

$$\varphi_{\mathrm{H_2}} = \exp\Big\{\exp(-3.8402T^{0.125} + 0.541)\,P - \exp(-0.1263T^{0.5} - 15.980)\,P^2 + 300[\exp(-0.011901T - 5.941)]\left[\exp\left(-\frac{P}{300}\right)\right]\Big\} \tag{8}$$

$$\varphi_{\mathrm{N_2}} = 0.93431737 + 0.3101804 \times 10^{-3}T + 0.295896 \times 10^{-3}P - 0.2707279 \times 10^{-6}T^2 + 0.4775207 \times 10^{-6}P^2 \tag{9}$$

$$\varphi_{\mathrm{NH_3}} = 0.1438996 + 0.2028538 \times 10^{-2}T - 0.4487672 \times 10^{-3}P - 0.1142945 \times 10^{-5}T^2 + 0.2761216 \times 10^{-6}P^2 \tag{10}$$

The nine constants in the above equations, k_0, α, w_2, w_3, n, A_X, and B_X (X = H_2 or NH_3), are determined by the least-squares method with the following optimization methods:

Step 1. Temporally substitute initial parameter values to the equations

Step 2. Simulate the reaction using the current parameters in the repeated steps. The instantaneous reaction rate is derived by Eq. (1). The reaction proceeds according to the obtained reaction rate, and the isothermal and isobaric gas ratio of N_2, H_2, and NH_3 is updated. One reaction step is assumed to be 1 msec. The reaction rate is recalculated by Eq. (1) based on the updated gas composition. These are repeated until the total reaction time reaches the estimated residence time. The obtained ammonia concentration $C_{NH_3}^{out}$ [%] are compared with the experimental results.

Step. 3. Update the nine constants to minimize the squares of errors between the simulation and experimental results of $C_{NH_3}^{out}$ in each experiment, and return to step 2.

Step. 4. Obtain final parameters when the difference in the cycle is lower than 10^{-8}

Trust Region Reflective Algorithm was utilized to determine the parameters in the least-squares method.[69] The obtained reaction kinetics were implemented by user Fortran subroutines of the Plug flow reactor (RPlug) model in Aspen Plus©, and the "RPlug" model was adopted in adiabatic conditions. The kinetics for KM1R and R/C were the same with our previous report.[70]

2.5 Economic analysis

The total cost for the loops is separated into a capital cost, C^{cap}, and an operation cost, C^{op}. C^{cap} was estimated by the following equations:[18]

$$C^{cap} = \sum_j C_j \tag{11}$$

$$C_j = \left(C_{j,fix} + LM \times\times AF \times C_{j,ref} \times \left(\frac{s_j}{s_{ref}} \right)^{n_j} \right) \times \frac{\text{CEPCI}}{1000} \quad (12)$$

C_j is the Bare Module Cost for equipment j. $C_{j,fix}$ is the cost of the control system of j. LM is the cost of Labor and materials. AF is an alloy factor, which is determined by the cost of materials. $C_{j,ref}$ is the cost for j in a reference scale, s_{ref}. s_j is the actual scale of j. n_j is a parameter that determines the influence of a scale. The parameters in equation (12) for each equipment, j, are given in Table 2 with the assumption that Chemical plant cost indexes (CEPCI) is 1000. Adjustment Factor in Table 3 is multiplied to the $C_{j,ref}$ (j = reactor or refrigerator) in a reference scale. Stainless steel (SUS 304) was employed for the material for reactors, compressors, and heat exchangers (shell and tube) with the alloy factor, 2.75 for reactors and compressors and 2.80 for heat exchangers.[18] It is because SUS 304 is durable for the temperature and the pressure required for the plants and is tolerant for hydrogen embrittlement.[71,72] CEPCI in 2019, 607.5 was utilized.

Table 2. Summary of the parameter for eq. (14)[18]

Unit	Basis	$C_{j,fix}$	$C_{j,ref}$	s_{ref}	n_j	LM	AF
Reactor	Volume（m^3)	63,000	110,000	20	0.52	2.30	2.75
Compressor, Low	Rated Power (kW)	7,000	1,350,000	1000	0.90	2.15	2.75
Compressor, High	Rated Power (kW)	7,000	10,300,000	10000	0.71	2.15	2.75
Heat Exchanger	Area (m^2)	27,000	70,000	100	0.71	2.80	2.80
Pump, small	Rated Power (kW)	7,000	7,000	16	0.26	1.47	1.90
Pump, large	Rated Power (kW)	7,000	7,000	16	0.43	1.47	1.90
Refrigerator	Rated Power (kW)	40,000	800,000	1,000	0.77	1.30	1.00

Table 3 Adjustment Factor for reactor and refrigerator

Equipment	Unit	Values	Adjustment Factor
Reactor	bar	150	3.4
	bar	100	2.3
	bar	75	1.9
	bar	50	1.6
	bar	30	1.3
	bar	10	1.0
Refrigerator	°C	−40	4.0
	°C	−51	7.0

C^{op} was calculated by the following equation:[18]

$$C^{op} = \sum_{t=1}^{year} \frac{1}{(1+d)^{t-1}} \left(P_{elec} E_{year} + P_{cat}\,(duration, t) \times BD \times V_{reactor} \right) \quad (13)$$

$$P_{cat}\,(duration, t) = \begin{cases} p_{cat}\,(duration = 1) \\ p_{cat}\,\left(duration > 1, t \equiv 1 (mod\ duration)\right) \\ 0\,\left(duration > 1, t \not\equiv 1 (mod\ duration)\right) \end{cases} \quad (14)$$

where *year*, the duration of the operation, is assumed as 20 years. With the assumption to implement the plant in the USA because of the available data, *d* is the discount rate, 2.25%.[73] P_{elec} is the cost for electricity and two patterns

are assumed: 0.0683 USD/kWh, the price for the industrial sector in 2019 in the USA,[74] and 0.273 USD/kWh the price for photovoltaics with rechargeable batteries (batteries 0.206 $/kWh + photovoltaics 0.067 $/kWh) under USA circumstance.[75] The required energy per year, E_{year}, is estimated by the output from Aspen Plus©.

The term "$P_{cat}\,(duration, t) \times BD \times V_{reactor}$" calculates the cost of catalyst used in the plant. The catalyst cost is generally estimated by weight and material cost per weight without the economy of scale.[76] $P_{cat}\,(duration, t)$ is the catalyst price [USD/kg] and is determined for each year by Eq. (14). $P_{cat}\,(duration, t)$ depends on the catalyst durability period (*duration*), and the cost is incurred when the catalyst is replaced. The influence of *duration* was evaluated by changing it from 1 to 10 years. *BD* is the bulk density of the catalyst used [g/cm^3] and $V_{reactor}$ is the volume of the reactor used in the ammonia synthesis loop [m^3]. The catalyst prices, bulk densities, and porosities of the four catalysts used in this study are summarized in the Table 4. *BD* of KM1R (iron-based catalyst)[60] and Ru/C[77] were obtained from literature values, while the bulk densities of the recent catalysts (Ru/Pr_2O_3 and Ru/Ba-Ca$(NH_2)_2$) were calculated to obtain a porosity of 0.60 when the catalyst is packed in the reactor.[4,60] The price of KM1R (iron-based catalyst) was set at 0.02 USD/g based on past transactions.[78] The cost of ruthenium-based catalyst, p_{cat} was calculated by multiplying the amount of ruthenium contained in the catalyst by the unit price of ruthenium (19 USD/g).[79]

Table 4 Price, bulk density, and porosity of the catalysts

Catalyst	Ru Content [wt%]	Price [USD/g]	Bulk Density [g/cm^3]	Porosity [-]
KM1R	-	0.020	2.80	0.52
Ru/C	3.2	0.608	0.80	0.63
Ru/Pr_2O_3	5	0.950	2.59	0.60
Ru/Ba-Ca$(NH_2)_2$	10	1.900	0.79	0.60

3. Results and discussion

3.1 Validation of simulated results

The parameter values obtained through the least-squares method are shown in Table 5. Figures 3 and 4 show $C_{NH_3}^{out}$ of experiments using Ru/Pr_2O_3 and Ru/Ba-Ca$(NH_2)_2$ and simulation results of a single pass over the reactor for validation based on the values in Table 5. In the case of Ru/Pr_2O_3, the simulation results approximately describe the experimental values, although the error tends to be significant at higher pressure conditions. As for Ru/Ba-Ca$(NH_2)_2$, the R^2 values of the fitting are high, and the modeling is sufficiently accurate at various reaction conditions. Thus, it was found that the Modified-Temkin model reproduces the experimental results for each of the new Ru-based catalysts, Ru/Pr_2O_3 and Ru/Ba-Ca$(NH_2)_2$, by parameter fitting through the least-squares method. It is the first example of modeling the reactions of Ru-based catalysts other than Ru/C with the Modified-Temkin equation, which considers the reverse reaction.

Figure 5 shows the $C_{NH_3}^{out}$ of Ru/Pr_2O_3 and Ru/Ba-Ca$(NH_2)_2$ at 10-50 bar, predicted by the extrapolation of the results under low pressures. The predictions assume that the temperature in the reactor is always constant (isothermal). The $C_{NH_3}^{out}$ reaches its peak at 350−450 °C, and the peak temperature increases at higher pressure. The equilibrium concentration of ammonia is reduced at higher temperature and increase at larger pressure. Then, the reaction rates in Fig. 5 is influenced by the chemical equilibrium in the high-temperature region. The order of catalytic activity is

$Ru/Ba\text{-}Ca(NH_2)_2$ > Ru/Pr_2O_3 > Ru/C in all pressure and temperature ranges (see Supplementary information).

Table 5 The parameter values obtained through the least-squares method. The values for KM1R and Ru/C are the same with our previous report.[70]

Catalyst	E_a (kJ/mol)	k_0	n	α	w_2	w_3	A_{H2}	B_{H2}	A_{NH3}	B_{NH3}
Ru/Pr_2O_3	101	1.13×10^{10}	0.21	0.10	0.10	0.10	15.4	509	17.7	424.0
$Ru/Ba\text{-}Ca(NH_2)_2$	59.4	8.64×10^{6}	0.73	0.10	0.18	0.10	5.9	8742	96.4	5073

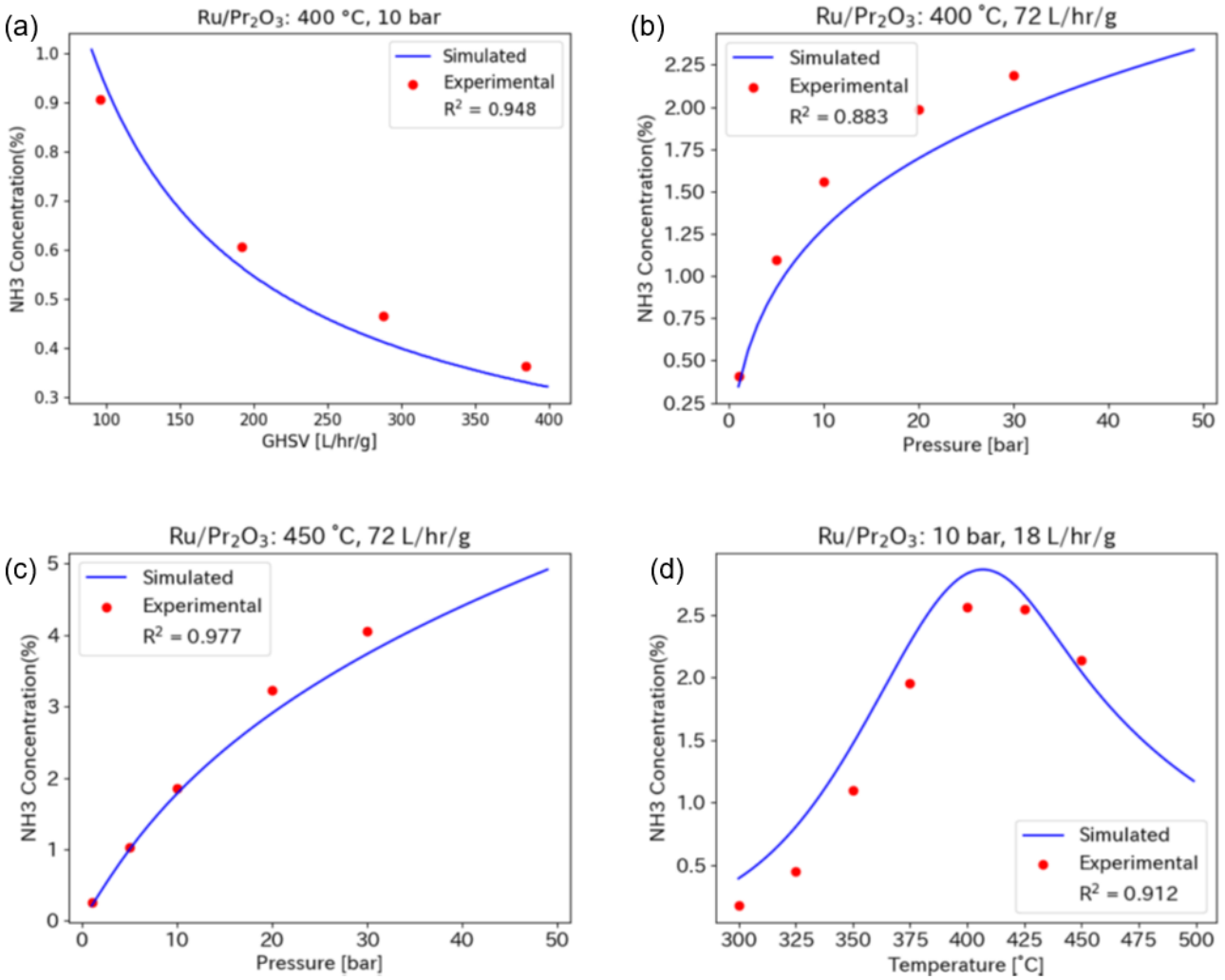

Figure 3 Experimental and simulated $C_{NH_3}^{out}$ of Ru/Pr_2O_3 against GHSV (a), pressure at 400 °C (b), pressure at 450 °C (c), and temperature (d).

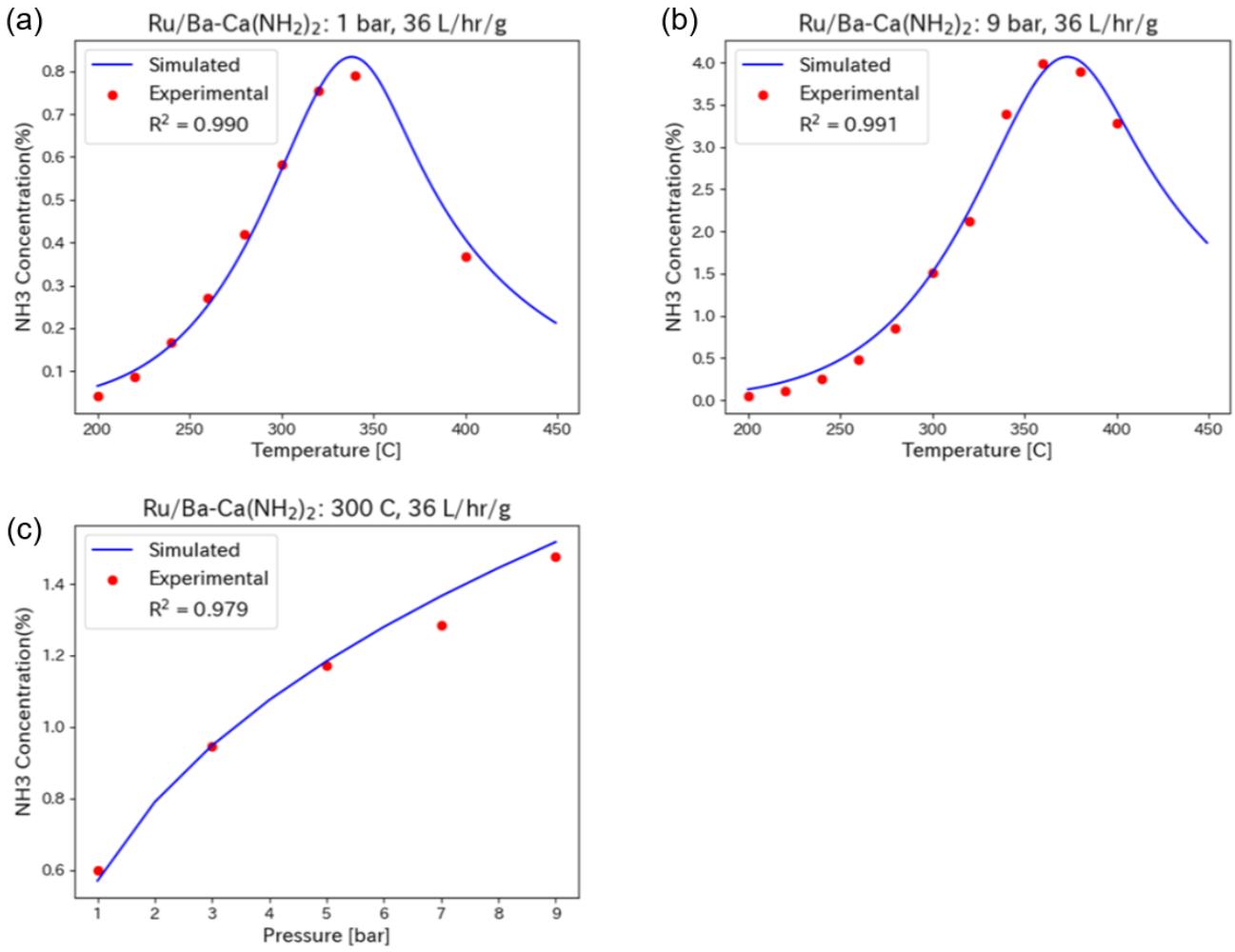

Figure 4 Experimental and simulated $C_{NH_3}^{out}$ of Ru/Ba-Ca$(NH_2)_2$ against temperature at 1 bar (a), the temperature at 9 bar (b), and pressure at 300 ℃ (c).

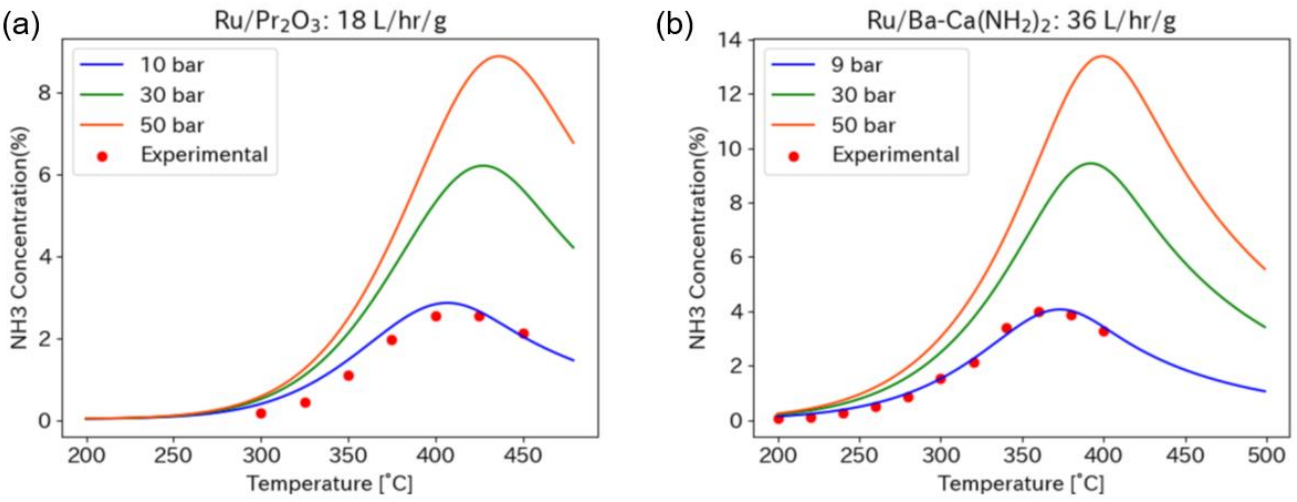

Figure 5 The $C_{NH_3}^{out}$ extrapolated until 50 bar over Ru/Pr_2O_3 and Ru/Ba-Ca$(NH_2)_2$

3.2 Overall cost of ammonia synthesis loop under low pressures with industrial electricity

First, to show reliable simulation results, the total cost was evaluated at 30 bar for Ru/Pr_2O_3 and 10 bar for $Ru/Ba\text{-}Ca(NH_2)_2$, near pressures to available experimental data. 0.0683 USD/kWh was utilized for the electricity cost. The total costs and their breakdown are shown in Figure 6. The operating conditions for each catalyst and pressure were optimized to achieve the lowest total cost (the case of 100 tonnes/day is shown in Table S1). As Figure 6 shows, the catalyst is the most expensive, even with 10-year catalyst durability. It is because the reported reaction rates under the mild conditions are not fast enough, and the reactor volume and the amount of catalyst required to fill it are too large. Considering the industrialization of ammonia synthesis catalysts, the reaction conditions published in the paper base should be a little closer to the industrial process.

At the small plant scale of 100 tonnes/day, the ratio of power cost to the total cost is more significant than that of equipment cost. Because of economies of scale in equipment costs, the percentage of equipment costs to the total expenses decreases further if a plant scale larger than 100 tonnes/day. The case that the plant scale is smaller than 100 tonnes/day is vice versa.

In addition, Ru/Pr_2O_3 and $Ru/Ba\text{-}Ca(NH_2)_2$ save electricity for compression of the introduced gas due to their low pressure. On the other hand, the low pressure makes liquefaction and recovery difficult, and as shown in Table S1, very low temperatures are required. In other words, the advantage of reduced power costs due to lower pressure reaction conditions is offset by the power necessary for lower temperatures in the recovery process. It is the same conclusion as our previous report.[70]

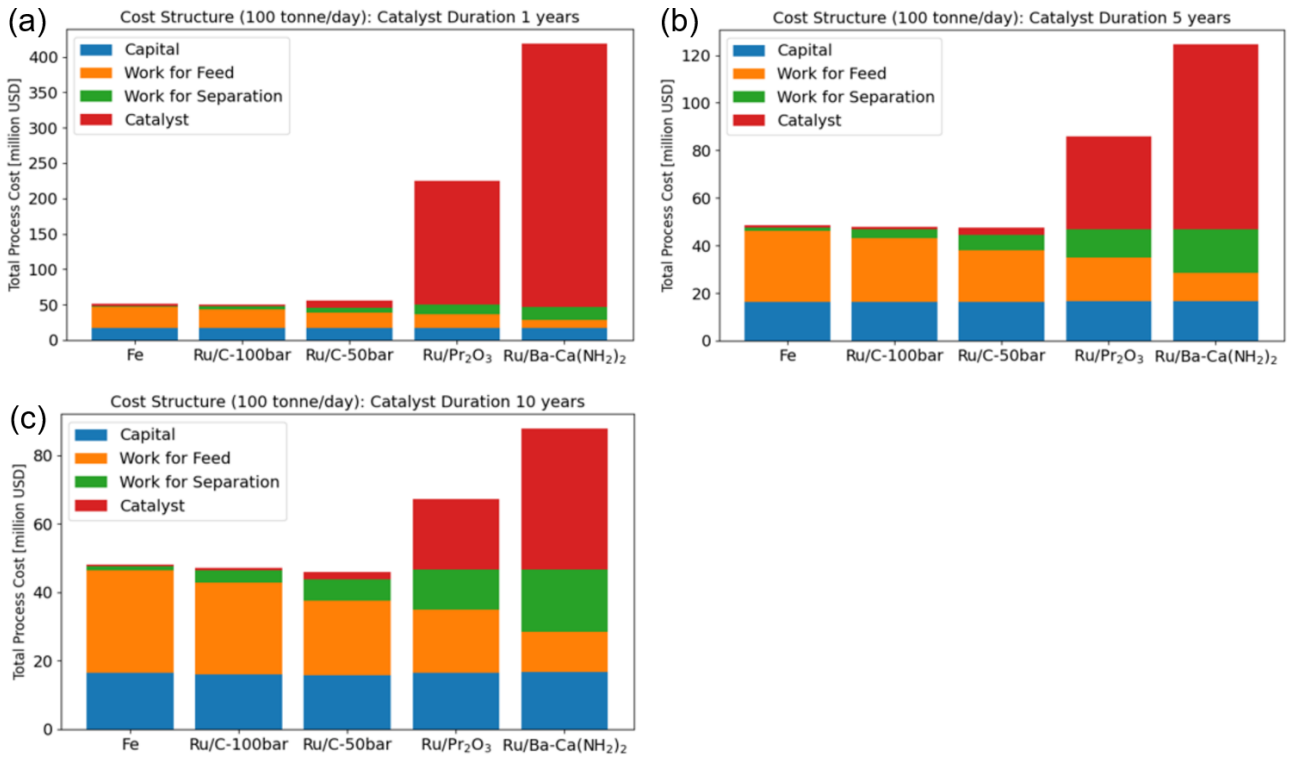

Figure 6 Breakdown of the cost of ammonia synthesis loop under low pressure for Ru/Pr_2O_3 and $Ru/Ba\text{-}Ca(NH_2)_2$ in different duration of catalyst at 100 tonnes/day scale.

3.3 Overall cost of ammonia synthesis loop under high pressures with industrial electricity

As shown in section 3.2, the experimental data reported in literature are unsuitable for practical use. Then, the extrapolated data of the reaction rate under 50 bar are utilized for the comparison. 0.0683 USD/kWh was utilized for the electricity cost. Figure 7 shows the breakdown of the total cost for the ammonia synthesis loop at a 100 tonnes/day scale. The high pressure significantly improved the reaction rate of Ru/Ba-Ca$(NH_2)_2$. If the duration of Ru/Pr_2O_3 and Ru/Ba-Ca$(NH_2)_2$ are 10 years, the total cost is comparable with conventional catalysts. Yet, the advantages of new catalysts are not these conditions.

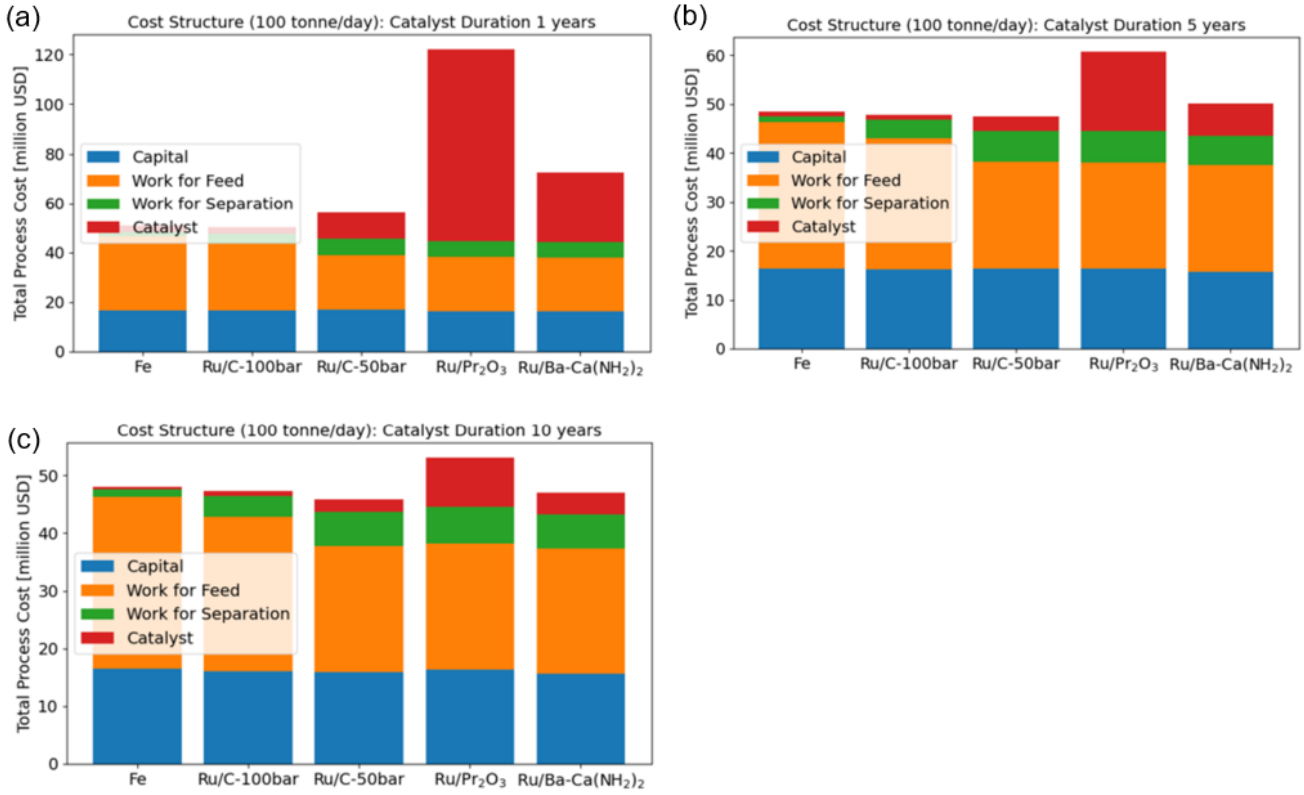

Figure 7 Breakdown of the cost of ammonia synthesis loop under high pressure for Ru/Pr_2O_3 and Ru/Ba-Ca$(NH_2)_2$ in different duration of catalyst at 100 tonnes/day scale.

3.4 Overall cost of ammonia synthesis loop under high pressures with photovoltaics and rechargeable battery

With the extrapolated data under 50 bar, we assumed that renewable energy is utilized to produce ammonia at a small scale locally: the production scale is 5 tonnes/day, and the electricity cost is 0.273 USD/kWh bearing photovoltaics and rechargeable battery. Figure 8 shows the breakdown of the total cost for the ammonia synthesis loop under the situation. If the durations of new catalysts are 10 years, the total cost of Ru/Ba-Ca$(NH_2)_2$ is smaller than conventional catalysts. Therefore, the new catalysts are advantageous if electricity is pretty high, the production scale is small, and the catalyst duration is long. The former two points are the characteristics of green ammonia synthesis, and thus the new catalysts are suitable for green ammonia production. The result when the electricity cost is 0.0683 USD/kWh at a 5 tonnes/day scale is shown in Supplementary Information, indicating lower price is not suitable for new catalysts.

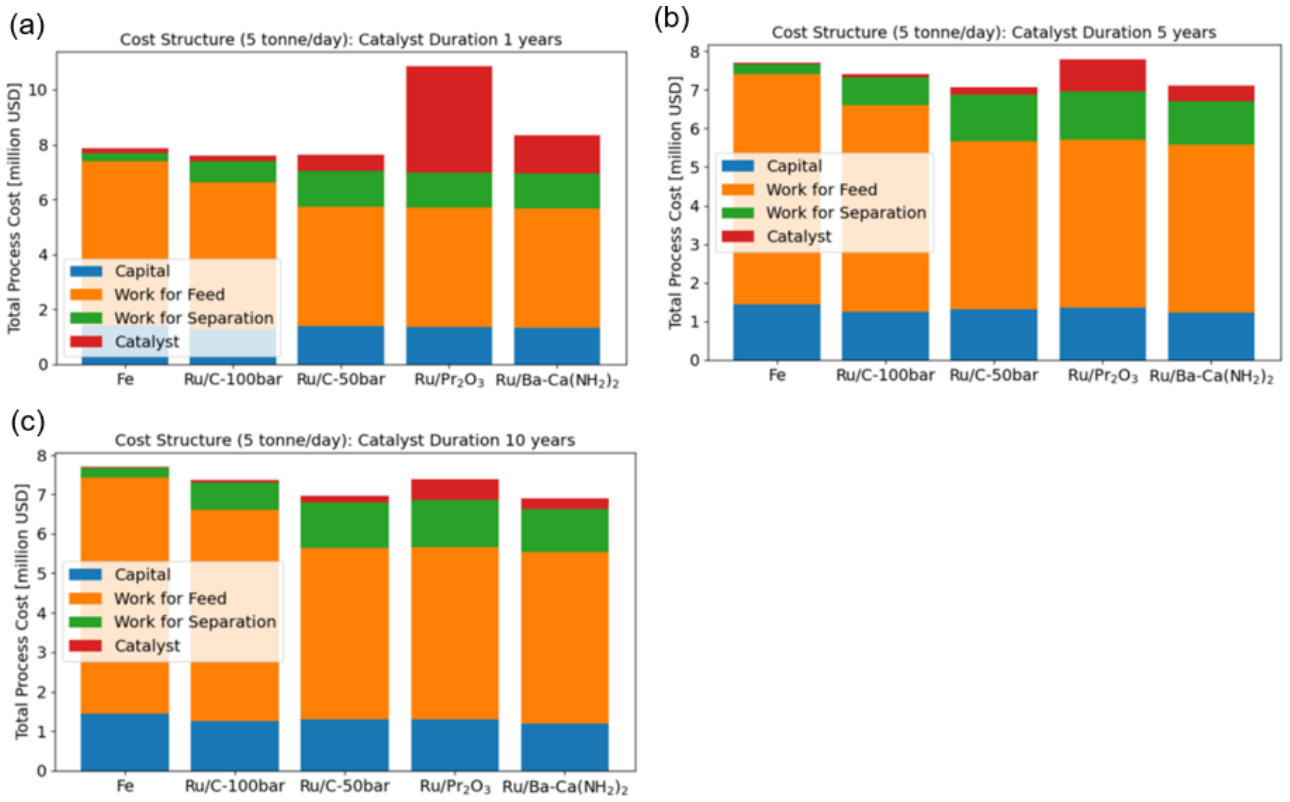

Figure 8 Breakdown of the cost of ammonia synthesis loop under high pressure for Ru/Pr_2O_3 and $Ru/Ba\text{-}Ca(NH_2)_2$ in different duration of catalyst at 5 tonnes/day scale.

3.5 Direction for the catalyst development and the limitation of this study

Based on the results, the newly developed catalysts are advantageous for green ammonia synthesis. However, it requires the long durability of the catalysts, such as 10 years. Meanwhile, we did not consider recycling or reactivating catalysts, which mitigate the catalyst cost. Therefore, the investigation of these processes will also be critical. Otherwise, the catalysts bearing cheap metal, such as Ni[25] or Co[80,81], effectively reduce the catalyst costs.

The advantage of low-pressure processes achieved by the new catalysts is not significant in terms of electricity consumption because the low pressure increases the power required for cooling and separation of synthesized ammonia. Instead of cooling separation, the separation method based on adsorbents such as alkali metal salts that selectively and reversibly absorbs ammonia is promising.[82,83] Since the absorption of ammonia occurs at around 200 °C, the synthesized gas does not need to be cooled to the temperature at which ammonia condenses, which will reduce the cost of compressors and heat exchangers. This study further clarifies the benefits of the mild reaction conditions achieved by the new catalyst.

4. Conclusion

We evaluated the cost of the ammonia synthesis loops embedded with $Ru/Ca(NH_2)_2$ and Ru/Pr_2O_3, newly developed and very active catalysts under mild conditions. The results elucidated that the cost for ruthenium is dominant, and the lifetime of catalysts is one of the critical parameters. Moreover, the new catalysts are advantageous for green ammonia synthesis: the case that the electricity price is high and the production scale is small. Finally, as the directions for further research, the results suggest reducing catalysts cost, such as the extension of catalyst lifetime,

recycling or reactivation of the catalysts, and substituting ruthenium with cheap metal.

Acknowledgment

This research was supported by the Environment Research and Technology Development Fund (JPMEERF20192R02) of the Environmental Restoration and Conservation Agency of Japan.

Author Contributions

† M. Y. and T. O. contributed equally to this work.

References

(1) Survey, U. S. G. *Mineral Commodity Summaries 2020*, 2020.

(2) Survey, U. S. G. *Mineral Commodity Summaries* **2020**, 116.

(3) Administration, U. S. E. I. **2020**.

(4) Liu, H. *Ammonia synthesis catalysts : innovation and practice*; Chemical Industry Press World Scientific, 2013.

(5) Lamb, K. E.; Dolan, M. D.; Kennedy, D. F. *Int. J. Hydrog. Energy* **2019**, *44*, 3580.

(6) Kojima, Y. *Int. J. Hydrog. Energy* **2019**, *44*, 18179.

(7) Lan, R.; Irvine, J. T. S.; Tao, S. *Int. J. Hydrog. Energy* **2012**, *37*, 1482.

(8) Wijayanta, A. T.; Oda, T.; Purnomo, C. W.; Kashiwagi, T.; Aziz, M. *Int. J. Hydrog. Energy* **2019**, *44*, 15026.

(9) Zhao, Y.; Setzler, B. P.; Wang, J.; Nash, J.; Wang, T.; Xu, B.; Yan, Y. *Joule* **2019**.

(10) Kobayashi, H.; Hayakawa, A.; Somarathne, K. D. Kunkuma A.; Okafor, Ekenechukwu C. *Proceedings of the Combustion Institute* **2019**, *37*, 109.

(11) Sgouridis, S.; Carbajales-Dale, M.; Csala, D.; Chiesa, M.; Bardi, U. *Nature Energy* **2019**.

(12) Götz, M.; Lefebvre, J.; Mörs, F.; McDaniel Koch, A.; Graf, F.; Bajohr, S.; Reimert, R.; Kolb, T. *Renewable Energy* **2016**, *85*, 1371.

(13) Supekar, S. D.; Skerlos, S. J. *Environ Sci Technol* **2015**, *49*, 12576.

(14) Ogawa, T. In *Emerging Trends to Approaching Zero Waste*; Hussain, C. M., Singh, S., Goswami, L., Eds.; Elsevier: 2022, p 265.

(15) Administration, U. S. E. I. *International Energy Outlook* **2016**, 127.

(16) Atkins, P. W.; De Paula, J.; Keeler, J. *Atkins' Physical Chemistry*; Oxford University Press, 2018.

(17) Liu, H. Z. *Chin. J. Catal.* **2014**, *35*, 1619.

(18) Woods, D. R. *Wiley-VCH Verlag GmbH & Co. KGaA* **2007**.

(19) Brown, D. E.; Edmonds, T.; Joyner, R. W.; McCarroll, J. J.; Tennison, S. R. *Catalysis Letters* **2014**, *144*, 545.

(20) Chauhan, M. *Nexant* **2018**, 1.

(21) Gro Intelligence: 2016; Vol. 2022.

(22) Gill, R. H. 1986; Vol. US4728506A.

(23) Paul J. FaustOtto C. Pless, J. 1978; Vol. US4171343A.

(24) Kitano, M.; Inoue, Y.; Yamazaki, Y.; Hayashi, F.; Kanbara, S.; Matsuishi, S.; Yokoyama, T.; Kim, S. W.; Hara, M.; Hosono, H. *Nat. Chem.* **2012**, *4*, 934.

(25) Ye, T.-N.; Park, S.-W.; Lu, Y.; Li, J.; Sasase, M.; Kitano, M.; Tada, T.; Hosono, H. *Nature* **2020**, *583*, 391.

(26) Ogawa, T.; Kobayashi, Y.; Mizoguchi, H.; Kitano, M.; Abe, H.; Tada, T.; Toda, Y.; Niwa, Y.; Hosono, H. *J. Phys. Chem. C* **2018**, *122*, 10468.

(27) Hattori, M.; Mori, T.; Arai, T.; Inoue, Y.; Sasase, M.; Tada, T.; Kitano, M.; Yokoyama, T.; Hara, M.; Hosono, H. *ACS Catal.* **2018**, 10977.

(28) Wang, P.; Chang, F.; Gao, W.; Guo, J.; Wu, G.; He, T.; Chen, P. *Nat Chem* **2017**, *9*, 64.

(29) Wang, Q.; Pan, J.; Guo, J.; Hansen, H. A.; Xie, H.; Jiang, L.; Hua, L.; Li, H.; Guan, Y.; Wang, P.; Gao, W.; Liu, L.; Cao, H.; Xiong, Z.; Vegge, T.; Chen, P. *Nature Catalysis* **2021**, *4*, 959.

(30) Kobayashi, Y.; Tang, Y.; Kageyama, T.; Yamashita, H.; Masuda, N.; Hosokawa, S.; Kageyama, H. *J Am Chem Soc* **2017**, *139*, 18240.

(31) Wu, J.; Li, J.; Gong, Y.; Kitano, M.; Inoshita, T.; Hosono, H. *Angew Chem Int Ed Engl* **2019**, *58*, 825.

(32) Yandulov, D. V.; Schrock, R. R. *Science* **2003**, *301*, 76.

(33) Wickramasinghe, L. A.; Ogawa, T.; Schrock, R. R.; Müller, P. *J. Amer. Chem. Soc.* **2017**, *139*, 9132.

(34) Arashiba, K.; Miyake, Y.; Nishibayashi, Y. *Nat. Chem.* **2011**, *3*, 120.

(35) Ashida, Y.; Arashiba, K.; Nakajima, K.; Nishibayashi, Y. *Nature* **2019**, *568*, 536.

(36) Anderson, J. S.; Rittle, J.; Peters, J. C. *Nature* **2013**, *501*, 84.

(37) Chalkley, M. J.; Drover, M. W.; Peters, J. C. *Chem Rev* **2020**.

(38) Nosherwani, S. A.; Neto, R. C. *Journal of Energy Storage* **2021**, *34*, 102201.

(39) Frattini, D.; Cinti, G.; Bidini, G.; Desideri, U.; Cioffi, R.; Jannelli, E. *Renewable Energy* **2016**, *99*, 472.

(40) Sánchez, A.; Martín, M. *Sustainable Production and Consumption* **2018**, *16*, 176.

(41) Sánchez, A.; Martín, M. *Journal of Cleaner Production* **2018**, *178*, 325.

(42) Al-Zareer, M.; Dincer, I.; Rosen, M. A. *Journal of Cleaner Production* **2018**, *196*, 390.

(43) Hasan, A.; Dincer, I. *Journal of Cleaner Production* **2019**, *231*, 1515.

(44) Bicer, Y.; Dincer, I.; Zamfirescu, C.; Vezina, G.; Raso, F. *Journal of Cleaner Production* **2016**, *135*, 1379.

(45) Araújo, A.; Skogestad, S. *Computers & Chemical Engineering* **2008**, *32*, 2920.

(46) Arora, P.; Hoadley, A. F. A.; Mahajani, S. M.; Ganesh, A. *Ind. Eng. Chem. Res.* **2016**, *55*, 6422.

(47) Andersson, J.; Lundgren, J. *Applied Energy* **2014**, *130*, 484.

(48) Kitano, M.; Inoue, Y.; Sasase, M.; Kishida, K.; Kobayashi, Y.; Nishiyama, K.; Tada, T.; Kawamura, S.; Yokoyama, T.; Hara, M.; Hosono, H. *Angewandte Chemie International Edition* **2018**.

(49) Imamura, K.; Miyahara, S.-i.; Kawano, Y.; Sato, K.; Nakasaka, Y.; Nagaoka, K. *Journal of the Taiwan Institute of Chemical Engineers* **2019**, *105*, 50.

(50) Tsubame BHB Co., L. 2022; Vol. 2022.

(51) Aika, K.; Ozaki, A.; Hori, H. *J. Catal.* **1972**, *27*, 424.

(52) Saadatjou, N.; Jafari, A.; Sahebdelfar, S. *Chem. Eng. Commun.* **2015**, *202*, 420.

(53) Aika, K.-i. *Catal. Today* **2017**, *286*, 14.

(54) Smith, A. R.; Klosek, J. *Fuel Processing Technology* **2001**, *70*, 115.

(55) Rohr, B. A.; Singh, A. R.; Nørskov, J. K. *J. Catal.* **2019**, *372*, 33.

(56) Aspen Technology, I. **2008**.

(57) Khademi, M. H.; Sabbaghi, R. S. *Chemical Engineering Research and Design* **2017**, *128*, 306.

(58) Nicol, W.; Hildebrandt, D.; Glasser, D. *Developments in Chemical Engineering and Mineral Processing* **1998**, *6*, 41.

(59) Liu, H. *Ammonia Synthesis Catalysts: Innovation and Practice*; World Scientific Publishing Company Pte Limited, 2013.

(60) Dyson, D. C.; Simon, J. M. *Industrial & Engineering Chemistry Fundamentals* **1968**, *7*, 605.

(61) Guacci, U.; Traina, F.; Ferraris, G. B.; Barisone, R. *Industrial & Engineering Chemistry Process Design and Development* **1977**, *16*, 166.

(62) Temkin, M. *Russian Journal of Physical Chemistry A* **1950**, *24*, 1312.

(63) Rossetti, I.; Pernicone, N.; Ferrero, F.; Forni, L. *Ind. Eng. Chem. Res.* **2006**, *45*, 4150.

(64) Rosowski, F.; Hornung, A.; Hinrichsen, O.; Herein, D.; Muhler, M.; Ertl, G. *Applied Catalysis A: General* **1997**, *151*, 443.

(65) Buzzi Ferraris, G.; Donati, G.; Rejna, F.; Carrà, S. *Chemical Engineering Science* **1974**, *29*, 1621.

(66) Gillespie, L. J.; Beattie, J. A. *Physical Review* **1930**, *36*, 743.

(67) Shaw, H. R.; Wones, D. R. *American Journal of Science* **1964**, *262*, 918.

(68) Newton, R. H. *Industrial & Engineering Chemistry* **1935**, *27*, 302.

(69) Yuying, L. *Centering, Trust Region, Reflective Techniques for Nonlinear Minimization Subject to Bounds*, 1993.

(70) Yoshida, M.; Ogawa, T.; Imamura, Y.; Ishihara, K. N. *Int. J. Hydrog. Energy* **2021**, *46*, 28840.

(71) Ashby, M. **2009**.

(72) Committee of Stainless Steel Producer, A. I. a. S. I. **1978**.

(73) Fund, I. M.; Vol. 2022.

(74) Administration, U. S. E. I. *Independent Statistics & Analysis* **2020**.

(75) Comello, S.; Reichelstein, S. *Nat Commun* **2019**, *10*, 2038.

(76) Peters, M. S.; Timmerhaus, K. D.; West, R. E. *Plant Design and Economics for Chemical Engineers*; McGraw-Hill Education, 2003.

(77) Rossetti, I.; Forni, L. *Applied Catalysis A: General* **2005**, *282*, 315.

(78) Corporation, Z.; Vol. 2022.

(79) umicore 2020.

(80) Sato, K.; Miyahara, S.-i.; Tsujimaru, K.; Wada, Y.; Toriyama, T.; Yamamoto, T.; Matsumura, S.; Inazu, K.; Mohri, H.; Iwasa, T.; Taketsugu, T.; Nagaoka, K. *ACS Catal.* **2021**, *11*, 13050.

(81) Inoue, Y.; Kitano, M.; Tokunari, M.; Taniguchi, T.; Ooya, K.; Abe, H.; Niwa, Y.; Sasase, M.; Hara, M.; Hosono, H. *ACS Catal.* **2019**, *9*, 1670.

(82) Wagner, K.; Malmali, M.; Smith, C.; McCormick, A.; Cussler, E. L.; Zhu, M.; Seaton, N. C. A. *AIChE Journal* **2017**, *63*, 3058.

(83) Malmali, M.; Le, G.; Hendrickson, J.; Prince, J.; McCormick, A. V.; Cussler, E. L. *ACS Sustainable Chemistry & Engineering* **2018**, *6*, 6536.